INTERNATIONAL JOURNAL OF PRECISION ENGINEERING AND MANUFACTURING Vol. 17, No. 9, pp. 1093-1099 SEPTEMBER 2016 / 1093
DOI: 10.1007/s12541-016-0133-6 ISSN 2234-7593 (Print) / ISSN 2005-4602 (Online)

Multi-Beam Angle Sensor for Flatness Measurement of Mirror using Circumferential Scan Technology

Meiyun Chen[1,#], Satoru Takahashi[2], and Kiyoshi Takamasu[1]

1 Faculty of Engineering, Department of Precision Engineering, The University of Tokyo, 7-3-1 Hongo, Bunkyo-ku, Tokyo, 113-8656, Japan
2 Research Center for Advanced Science and Technology, The University of Tokyo, 4-6-1 Komaba, Meguro-ku, Tokyo, 153-8904, Japan
Corresponding Author / E-mail: chenmeiyun@nanolab.t.u-tokyo.ac.jp, TEL: +81-03-5841-6472, FAX: +81-03-5841-6472

KEYWORDS: Micro-FMM, Multi-beam angle sensor, Flatness, Autocollimator, Stage-independence

Flatness tolerance of mirror is usually determined for a particular manufactured product based on the user's requirement. To help meet this requirement, we here propose a high-accuracy microscale flatness-measuring machine (micro-FMM) that consists of a multi-beam angle sensor (MBAS). We review the techniques and the sensors predominantly used in the industry to quantify flatness. Compared with other methods, the MBAS can eliminate zero-difference error by circumferential scan and automatically eliminates the tilt error caused by the rotation of a workpiece. Our optical probe uses the principle of an autocollimator, and the flatness measurement of the mirror comprises two steps. First, the MBAS is designed to rotate around a circle with a given radius. The workpiece surface profile along this trajectory is then measured by the micro-FMM. Experimental results, confirming the suitability of the MBAS for measuring flatness are also presented.

Manuscript received: January 21, 2016 / Revised: May 2, 2016 / Accepted: May 3, 2016

1. Introduction

Surface flatness of mirror is a critical feature in many industrial and commercial devices and instruments. A flat surface often serves as a reference against which to inspect other workpieces. The ISO 1101[1] standard for flatness tolerance quantifies flatness in terms of the space bounded by two parallel planes separated by *t*. This distance must meet application-specific requirements.[2]

Surface flatness of mirror can be assessed in various ways, some similar to straightness. A traditional approach involves sweeping the test surface in several places with a straight edge and observing where and how much light leaks through the contact region. This method suffers from any deviation in the straightness of the edge and from the diffraction of any light transmitted through even a very small gap. The edge must also be rotated on the surface to ensure true planarity.[3] Other techniques of measuring flatness such as coordinate-measuring machines (CMM) , the least-square arithmetic was applied in flatness based on CMM,[4] but there is a discrepancy in assessment the uncertainty, such as in referents.[5-7] Optical measurement methods have also been reported,[8-10] some based on interferometry.[11,12] However, interferometry technique is viable and does produce, under certain conditions, absolute values. Yokoyama proposed a novel interferometric measurement method using two heterodyne shearing interferometers.[13] Although this technique is robust and precise under general environment, the measurement curvature-range is limited, as the variation of curvature is not allowed to be too high.

Another technique, involving the use of an autocollimator,[14-17] yields notoriously high resolution and accuracy. When applied to a large work piece, many sensors are normally used to determine position coordinates. The scanning multi-probe system, consisting of two probe units of the three-probe method, whose straightness profile was evaluated with an accuracy of approximately 0.4 μm over a measurement length of 600 mm.[18] This widely used technique face the problem of the zero difference error; they carried out an accurate zero-adjustment by two probe-units (six sensors). This poses a problem that the probe non-linearity error (the main error sources) will generate in the zero-adjustment.[18]

Ikumatsu proposed the circumferential scan technique (used three displacement sensors) to measure the flatness, which verified can automatically reduce the zero-difference error.[19,20] However he only shows results of this study through theoretical analysis.

We therefore designed and built a simple but accurate small-angle generator using a multi-beam angle sensor (MBAS). Its dimensions are 125(L) mm × 130(W) mm × 90(H) mm. The flatness measurement of

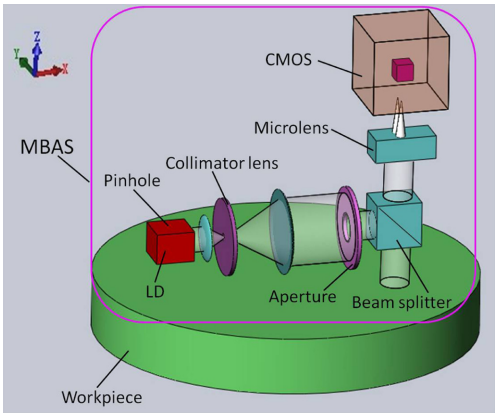

Fig. 1 Construction of the MBAS

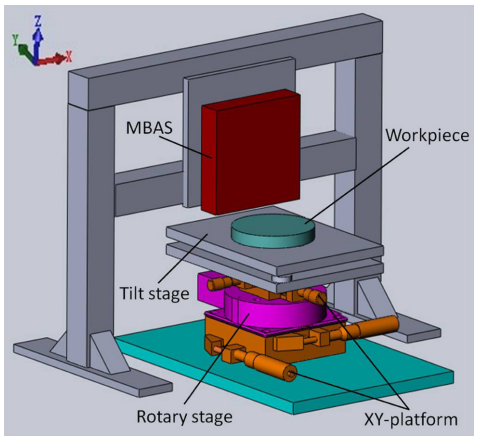

Fig. 2 Schematic of the micro-FMM: multi-beam angle sensor (MBAS), tilt stage, rotary unit, XY-platforms, and a support structure for holding the MBAS

the mirror comprises two steps. First, the MBAS is designed to rotate around a circle with a given radius. The workpiece surface profile along this trajectory is then measured by the micro-FMM. Compared with other methods, the MBAS can eliminate zero-difference error by circumferential scan and automatically eliminates the tilt error caused by the rotation of a workpiece. Experimental results, confirming the suitability of the MBAS for measuring flatness are also presented.

2. Micro-FMM Configuration

An autocollimator is an optical instrument that performs non-contact angle measurements at a reflecting surface. The MBAS is based on a multi-autocollimator system using microlenses to measure deflections in an optical system. It works by projecting an image onto a beam splitter, and measuring the deflection of the light reflected from the surface. The deflection of the light reflected at several points on the surface can be measured with a sensor. Then, the sensor is scanning the workpiece while it is rotating.

Fig. 1 illustrates the MBAS optical system. The laser beam from a

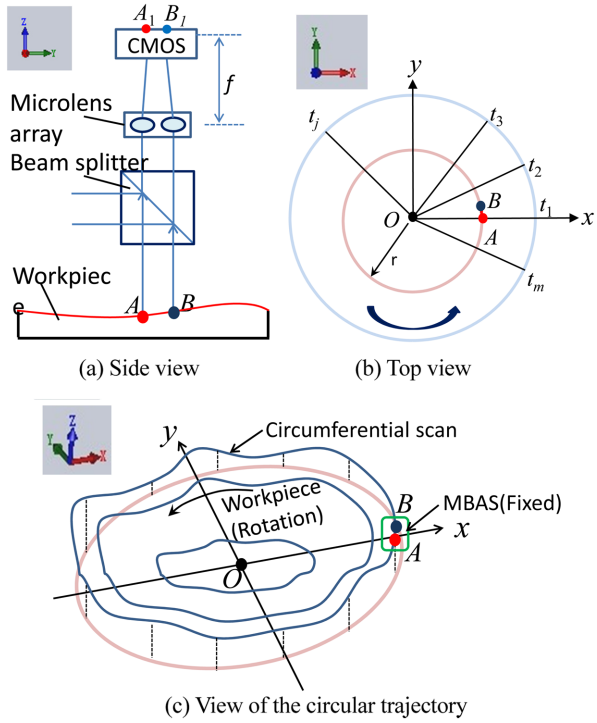

Fig. 3 Profile measurement along the circumference of a circle of radius *r*: the multi-beam angle sensor is fixed onto the support structure and scanning the workpiece while it is rotating. (a) Side view. (b) Top view. (c) Overall view of the measurement scans on concentric circles

laser diode (LD) passes through a pinhole and is collimated by a collimator lens. The beam is then reflected by a beam splitter and projected onto the workpiece surface. All of the beam reflected from the workpiece surface traverses the beam splitter to reach the microlens. After being focused by the microlens, it is split into several beams. The resulting pattern is observed and recorded by a CMOS camera oriented vertically, and the imaging can be observed on a TV monitor. Further processing of the pattern is carried out on a PC.

We used an MBAS to construct the experimental system shown in Fig. 2. A workpiece was placed on the tilt stage and the rotary platform was mounted between two XY-platforms. Thus, the rotary table acts as a small-angle generator and serves to set the reference position for the angle measurements. The MBAS was arranged to rotate around the circumference of a circle from the rotational center point. We then measured the workpiece surface profile along the circle by rotating the workpiece in increments.

3. Principle of the MBAS

3.1 Measurement of the angle difference *c*

The measurement of the angle difference involves two steps. First, the MBAS is placed so as to rotate around the circumference of a circle of radius *r* centered on point *O* on the workpiece surface. Then, the workpiece surface profile is measured along the circumference by rotating the workpiece in increments, as shown in Fig. 3. The workpiece flatness is determined in these two steps by the proposed algorithm.

Further details will be given in Section 4. One commonly used method for assessing surface flatness uses three sensors[18] that can measure distances relative to a fixed internal reference plane. However, this method is susceptible to tilt error and zero-difference error, i.e., discrepancies between the zero values of each sensor. The MBAS was designed to address this problem by eliminating the significance of the zero-difference error (Fig. 3) and automatically eliminating the significance of the tilt error that originates from the rotation of the workpiece (Fig. 5).

The MBAS uses a CMOS to capture the spot pattern produced by a microlens. See Fig. 3(a) for a schematic of the side view of the flatness measurement system. Here, f is the focal distance of the microlens and r the radius of measurement.

In the XY plane (Fig. 3(b)), the workpiece is rotated in angular increments of $\grave{e}$, with the MBAS initially oriented perpendicular to the x axis. Flatness is then measured along the straight line passing through the center of rotation, O. Fig. 3(c) illustrates how the two points A and B in the circumference of the circle of radius r are carried out by rotating the workpiece step by step.[19] The workpiece flatness is calculated by applying the autocollimator principle of the angle difference at each of these two angles on the workpiece. The angle difference can be calculated from the intensity distribution of the spots on the CMOS.[21] Then, the specimen profile at each location on the circle can be determined accurately. This procedure is repeated for circular scans of different radii, to yield the overall shape of the surface.

In the flatness measurement, the profile P can be denoted as the second order integration of the angle differential output c (the mathematical algorithm is shown in section 3.2), if the zero difference error c_0 is zero (the difference between the zero-value of the two angles will generate an offset c_0 in the angle differential output). However, if the c_0 is not equated zero, the second order integration of the offset c_0 will yield a quadratic curve in the profile evaluation. Generally known is the use of the three sensors for the purpose of determining the flatness of a surface. This widely used technique also face this problem, they carried out an accurate zero-adjustment by two probe-units (six sensors). This poses a problem that the probe non-linearity error (the main error sources) will generate in the zero-adjustment.[18]

In order to circumvent the problem of the zero-difference error mentioned in the last paragraph, we proposed the circumferential scan technique. Through one circumferential scanning (rotate 360 degree), suppose the first and last position is the same one, by the proposed algorithm (Fourier transform), which can automatically reduce the influence of zero-difference error. Ikumatsu also proposed the circumferential scan technique (used three displacement sensors) to measure the flatness, which verified can automatically reduce the zero-difference error.[19]

Fig. 4 outlines the principle of the angle-difference measurement by the MBAS. A_1 and B_1 are representative points on the workpiece at the rotation angle t_1 (as shown in the Fig. 3(b)), and c_{a1} and c_{b1} are the corresponding angles. Then, c is the angle difference between points A_1 and B_1. Here, A_0 and B_0 represent predetermined surface location of the points A_1 and B_1, and c_{a0} and c_{b0} are the corresponding angles. When the separation between A_1 and B_1 changes from x_0 to x_1, the relationship between the surface gradient in the Y direction and the reflected beams must be determined.

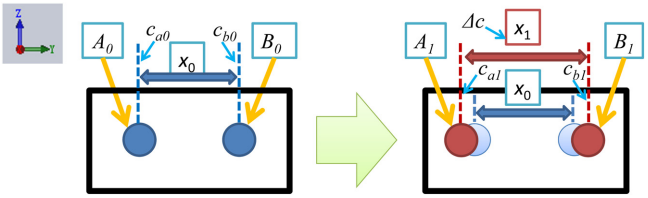

Fig. 4 Calculation of the angle difference from the intensity distribution of the center of the overall intensity distribution

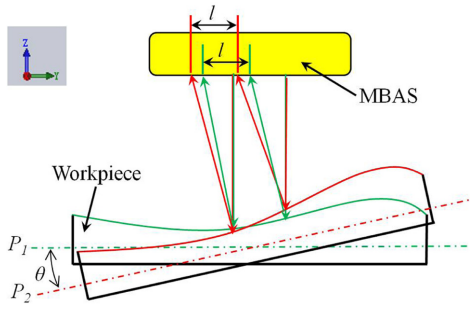

Fig. 5 Relation between surface curvature in the Y direction and the reflected beams: the green and red lines denote, respectively, the reference and the actual plane, tilted by angle $\grave{e}$ and the distance between the two reflected laser beams from P_1 plane is l

The MBAS is based on the autocollimator principle. An autocollimator measuring the distance between two reflected beams, which provides a measure of the angle difference of the workpiece. Assume that, as shown in Fig. 5, the green and red beams originate from planes P_1 and P_2, respectively. The distance between the two reflected laser beams from P_1 plane is l. When the surface tilts in the Y direction by an angle θ from plane P_1 to P_2, the positions of the two reflected beams from plane P_2 also changes. Relative to the reference plane P_1, plane P_2 is tilted by an angle θ, but the distance between the two reflected beams remains equal to l. Similar to autocollimators, the distance l provides a measure of the angle difference. Thus, the angle difference is unchanged by a change in gradient in the Y direction. The tilt error caused by the rotation is therefore negligible and the specimen profile can be measured accurately on each concentric circle.

3.2 Calculating the profile P from the angle difference *c*

Fig. 6 outlines the measurement algorithm. The profile P of a workpiece at a location t can be expressed as a Fourier series, given by

$$P(t_j) = a_0 + \sum_{i=1}^{n} (a_i \cos t_j i + b_i \sin t_j i) \quad t_j = \frac{2\pi(j-1)}{m} \qquad (1)$$

$$(j = 1, 2, \ldots, m)$$

where a_i and b_i are the Fourier series coefficients, n the maximum iterations of the Fourier series, and m the number of sample points. Here, the angle difference c can be measured by the sensor, and can also be expressed as the second order differential of the profile data P, given by

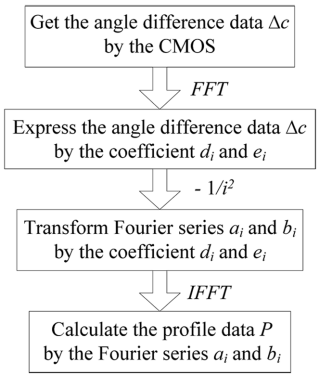

Fig. 6 Measurement flowchart: from the angle difference c to the profile data P via Fourier series

$$\Delta c(t_j) = P''(t_j) = -\sum_{i=1}^{n} i^2 (a_i \cos t_j i + b_i \sin t_j i) \tag{2}$$

Then, using a Fourier transformation, we can also transform the angle difference c to coefficients d_i and e_i, given by

$$c_j = \sum_{i=1}^{n} (d_i \cos t_j i + e_i \sin t_j i) = P''(t_j) \tag{3}$$

We note that the relationship between the Fourier series (a_i and b_i) and coefficients (d_i and e_i) can be denoted as

$$a_i = -\frac{d_i}{i^2}, \quad b_i = -\frac{e_i}{i^2} \tag{4}$$

Consequently, the profile P can be denoted as a Fourier series by using an inverse Fourier transform.

The characteristics of the algorithm can be estimated from its transfer function, which defines the relationship between the angle difference c and the profile data P.

Some simulation examples demonstrate how to calculate the roundness by using Fourier transform.[21] The simulation results also imply that the MBAS can measure roundness with repeatability under 10 nm if the random angle error is less than 0.8 μrad.

4. Pre-Experiment

4.1 Configuration of the pre-experiment

The pre-experimental arrangement is shown in Fig. 7. It consists of the MBAS (multi-autocollimator system with a microlens), two XY-platforms, a rotary platform, a tilt stage, and a support structure. We used a stage controller to move the rotary platform, controlled by Labview software on a PC, and recorded the MBAS output signals at each position.

Fig. 8 shows the constructed MBAS. A 650-nm-wavelength laser beam from a LD passes through a pinhole of diameter 400 μm and is collimated by the collimator lens. The beam is then reflected by a beam splitter and projected onto the workpiece surface. The reflected beam from the workpiece surface passes totally through the beam splitter and focuses it on the microlens, which divides the beams into several beams. Finally, the CMOS tracks the position of 8¥8 focal spots. The pitch of the microlens is 500 μm.

The resulting pattern is observed and recorded by the CMOS camera, oriented vertically. Table 1 lists the device specifications. The angle difference can be calculated from the intensity distribution.[21]

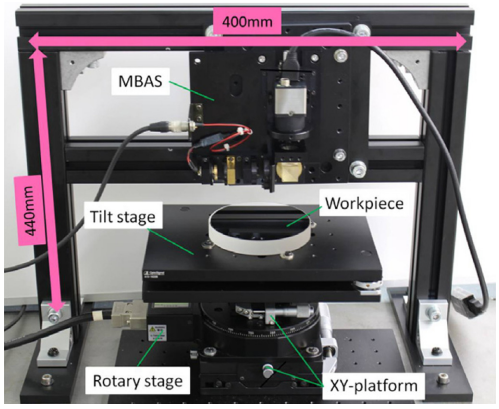

Fig. 7 Microscale flatness measurement setup, consisting of the MBAS, two XY platforms, a rotary platform, a tilt stage, and a supporting structure for the MBAS

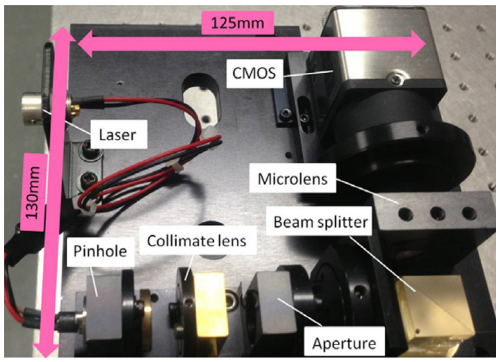

Fig. 8 Construction of the multi beam angle sensor: the MBAS is based on a multi-autocollimator system using a microlens

Table 1 Multi-beam angle sensor specifications (Fig. 8)

Laser Diode	Output power : 35 mW (CW) Wavelength : 658 nm
Pinhole	Diameter : 400 μm
Aperture	Diameter : 4 mm
Microlens	Focal distance : 46.7 mm (f) Pitch of the array : 500 μm
CMOS	Size : 5.6 mm × 4.2 mm Pixel size : 2.2 μm × 2.2 μm

4.2 MBAS stability

To verify the standard deviation of the MBAS measurements taken in a real environment, we measured the stability of the angles and the angle difference over two hours. Fig. 9 plots the angle measurements at points A and B, while the workpiece was not rotating. MBAS stability is then expressed as the standard deviation of the autocollimator output.

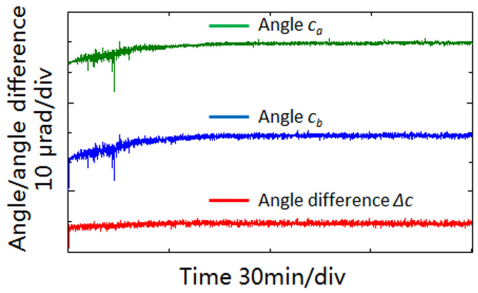

Fig. 9 MBAS stability: the angles and the angle difference were measured over two hours

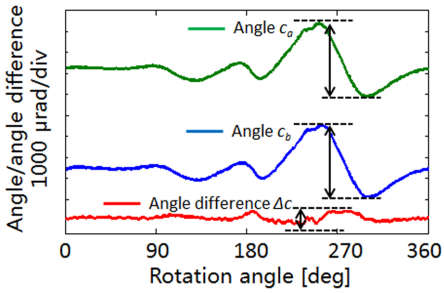

Fig. 10 Measured angles at points A and B and angle difference data for a PVC plate

Table 2 Experimental conditions

Parameters	Values
Radius of measurement	10 mm
Sample points	360
Rotation increment	1 degree

The experimental setup is mounted on a table in a basement. In Fig. 9, the long measurement time reveals a large thermal drift. The standard deviation for ca is 2.45 μrad, but that of c is 0.79 μrad. Here, the standard deviation c is the stability of the MBAS. We note that the fluctuation in the stability of c is small because it eliminates thermal drift. We therefore only consider the differential output to measure flatness.

Our stability testing demonstrates that a simple optical-path design makes the setup insensitive to environmental fluctuations.

4.3 Pre-experiment results

Mirrors were used as specimens in the experiment. Table 2 shows the experimental conditions. The workpiece is polyvinyl chloride (PVC) mirror coated with aluminum. The flatness of the coated PVC plate is of the order of several dozen micrometers.

Fig. 10 plots c_a, c_b, and c for the PVC plate, measured by the MBAS system, as functions of the rotation angle. The range of angle and angle difference of the rotation angle over 360 degree for the specimen are 3550 and 390 μrad, respectively. Measurements plotted in Fig. 11(a) show that the average flatness, measured over five trials, was 54.32 μm with average standard deviation of 52 nm (Fig. 11(b)).

To evaluate the MBAS method using real datasets, an experiment was developed using conventional high-precision machines (MITUTOYO FALCIO707) to measure the same PVC plate. Its flatness profile is plotted in Fig. 12 and has a flatness of 56.4 μm. Here, the indication accuracy of the MITUTOYO FALCIO707 is (1.9+4L/1000) μm, L is the measuring length (mm).

Fig. 12 shows the profile of the same workpiece obtained by two separate measurement methods. The flatness derived by the MBAS method and CMM are 54.32 and 56.4 μm, respectively. The MBAS measurement was done without any temperature control or vibration isolation.

From the results, it can be clearly seen that the MBAS measuring results follow the CMM very well in the whole. However, there is a slight difference in the measurements especially in some point elements (e.g. peaks, pits, saddle points) compared the two measuring results for

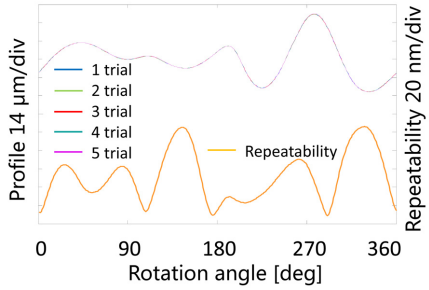

Fig. 11 Profile data (five trials) and repeatability (average standard deviation of five trials) test for a PVC plate measured with the MBAS

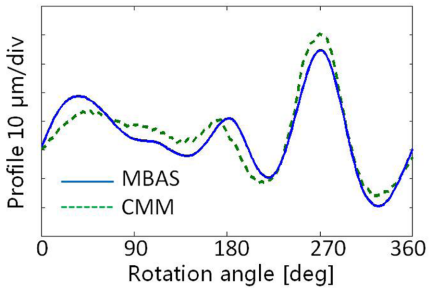

Fig. 12 Comparison of MBAS with CMM measurements

the following reasons: (1) the accuracy of the CMM is over 1.9 μm for limited range; (2) although we have measure the same PVC plate, the measuring position is not exactly same; and (3) MBAS is an optical instrument for non-contact measurement of angles, however, the CMM is using the contact sensor for measurement. Therefore, the measuring spot of the MBAS is larger than CMM.

To confirm the repeatability of the MBAS measurements, we repeated the experiment using a very flat mirror, with a flatness of several dozen nanometers.

Fig. 13 plots c_a and c_b for this mirror. The range of angle and angle difference of the rotation angle over 360 degree for the specimen are now 13.02 and 1.57 μrad, respectively. Profile data of the mirror are 76 nm with an average standard deviation 12 nm over four trials (Fig. 14).

The pre-experiment results (Table 3) confirm the suitability of the MBAS for measuring flatness. Future work will be necessary to

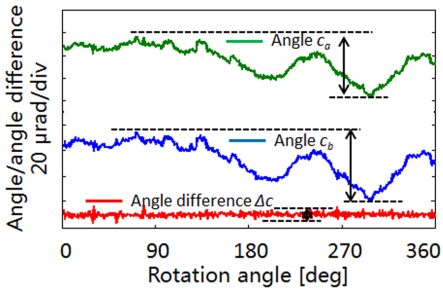

Fig. 13 Measured angles at points A and B, and the angle difference for the mirror

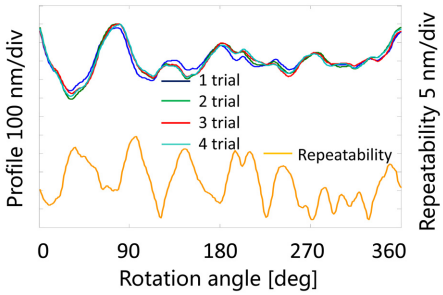

Fig. 14 MBAS profile data (four trials) and repeatability (standard deviation of four trials) test for the mirror

Table 3 Experimental results

Parameters	Plastic	Mirror
Flatness	54.32 μm	76 nm
Average STD	52 nm	12 nm

analyze the factors that influence the measurement accuracy and to find ways to assess and calibrate the MBAS.

5. Conclusions

We presented a new accurate microscale flatness-measuring machine (micro-FMM). This method uses only one probe, named the MBAS, to realize the precision flatness measurements. We verified that the MBAS can eliminate zero-difference error by circumferential scan and automatically eliminates the tilt error caused by the rotation of the workpiece when detecting angles. The MBAS can maintain high sensitivity with miniaturized size.

An MBAS system for measuring flatness was constructed. The optical probe is based on the principle of an autocollimator and has a stability of 0.79 μrad (the standard deviation of the angle difference).

The performance of the probe was confirmed experimentally. The flatness of a coated PVC plate was assessed by both the MBAS and CMM techniques, yielding 54.32 μm and 56.4 μm, respectively. Owing to the accuracy of the CMM, the discrepancy between the two techniques was 2.08 μm. Experimental results confirm the suitability of the MBAS for measuring flatness. To verify its repeatability, another experiment was done using a very flat mirror. This yielded a flatness of 76 nm with average standard deviation 12 nm, which hence verified the repeatability of the flatness measurements by MBAS.

A new experiment has been designed, which is planned to perform flatness measurement and analyze flatness measurement uncertainties. Although the repeatability of the MBAS is good enough, the flatness measurement and calibration the sensitivity of the MBAS will also be the future plan to execute.

ACKNOWLEDGEMENT

This research work was supported by the JSPS KAKENHI Grant number 26249006 and the program of China Scholarships Council (CSC).

REFERENCES

1. ISO 1101, “Geometrical Product Specifications (GPS) - Geometrical Tolerancing - Tolerances of Form, Orientation, Location and Run-Out,” 2012.
2. ISO 17450, “Geometrical Product Specifications (GPS) - General Concepts - Part 1: Model for Geometrical Specification and Verification,” 2011.
3. Whitehouse, D. J., “Handbook of Surface Metrology,” CRC Press, 1994.
4. Huang, M. F., Wang, Q. Y., Zhong, Y. R., Kuang, B., and Li, X. Q., “On the Flatness Uncertainty Estimation based on Data Elimination,” Applied Mechanics and Materials, Vols. 16-19, pp. 347-351, 2009.
5. Cui, C., Fu, S., and Huang, F., “Research on the Uncertainties from Different Form Error Evaluation Methods by Cmm Sampling,” The International Journal of Advanced Manufacturing Technology, Vol. 43, No. 1-2, pp. 136-145, 2009.
6. Choi, W. and Kurfess, T. R., “Uncertainty of Extreme Fit Evaluation for Three-Dimensional Measurement Data Analysis,” Computer-Aided Design, Vol. 30, No. 7, pp. 549-557, 1998.
7. Bachmann, J., marc Linares, J., Sprauel, J. M., and Bourdet, P., “Aide in Decision-Making: Contribution to Uncertainties in Three-Dimensional Measurement,” Precision Engineering, Vol. 28, No. 1, pp. 78-88, 2004.
8. Kolivand, H. and Sunar, M. S., “An Overview on Base Real-Time Shadow Techniques in Virtual Environments,” TELKOMNIKA (Telecommunication Computing Electronics and Control), Vol. 10, No. 1, pp. 171-178, 2012.
9. Kiyono, S., Asakawa, Y., Inamoto, M., and Kamada, O., “A Differential Laser Autocollimation Probe for On-Machine Measurement,” Precision Engineering, Vol. 15, No. 2, pp. 68-76, 1993.
10. Bünnagel, R., Oehring, H.-A., and Steiner, K., “Fizeau

Interferometer for Measuring the Flatness of Optical Surfaces," Applied Optics, Vol. 7, No. 2, pp. 331-335, 1968.

11. Hariharan, P., "Interferometric Testing of Optical Surfaces: Absolute Measurements of Flatness," Optical Engineering, Vol. 36, No. 9, pp. 2478-2481, 1997.
12. Kim, W. J., Shimizu, Y., Kimura, A., and Gao, W., "Fast Evaluation of Period Deviation and Flatness of a Linear Scale by using a Fizeau Interferometer," Int. J. Precis. Eng. Manuf., Vol. 13, No. 9, pp. 1517-1524, 2012.
13. Yokoyama, T., Yokoyama, S., Yoshimori, K., and Araki, T., "Sub-Nanometre Double Shearing Heterodyne Interferometry for Profiling Large Scale Planar Surfaces," Measurement Science and Technology, Vol. 15, No. 12, pp. 2435-2443, 2004.
14. Yoder, P., Schlesinger, E. R., and Chickvary, J., "Active Annular-Beam Laser Autocollimator System," Applied Optics, Vol. 14, No. 8, pp. 1890-1895, 1975.
15. Ennos, A. and Virdee, M., "High Accuracy Profile Measurement of Quasi-Conical Mirror Surfaces by Laser Autocollimation," Precision Engineering, Vol. 4, No. 1, pp. 5-8, 1982.
16. Schuda, F. J., "High-Precision, Wide-Range, Dual-Axis, Angle Monitoring System," Review of Scientific Instruments, Vol. 54, No. 12, pp. 1648-1652, 1983.
17. Luther, G. G., Deslattes, R. D., and Towler, W. R., "Single Axis Photoelectronic Autocollimator," Review of Scientific Instruments, Vol. 55, No. 5, pp. 747-750, 1984.
18. Gao, W., Yokoyama, J., Kojima, H., and Kiyono, S., "Precision Measurement of Cylinder Straightness using a Scanning Multi-Probe System," Precision Engineering, Vol. 26, No. 3, pp. 279-288, 2002.
19. Fujimoto, I., Nishimura, K., Takatsuji, T., and Pyun, Y.-S., "A Technique to Measure the Flatness of Next-Generation 450mm Wafers using a Three-Point Method with an Autonomous Calibration Function," Precision Engineering, Vol. 36, No. 2, pp. 270-280, 2012.
20. Fujimoto, I., Takatsuji, T., Nishimura, K., and Pyun, Y.-S., "An Uncertainty Analysis of Displacement Sensors with the Three-Point Method," Measurement Science and Technology, Vol. 23, No. 11, Paper No. 115102, 2012.
21. Chen, M., Takahashi, S., and Takamasu, K., "Development of High-Precision Micro-Roundness Measuring Machine using a High-Sensitivity and Compact Multi-Beam Angle Sensor," Precision Engineering, Vol. 42, pp. 276-282, 2015.